Morphology and Thermal Behavior of Organo-Bentonite Clay/Poly(styrene-*co*-methacrylic acid)/Poly(isobutyl methacrylate-*co*-4-vinylpyridine) Nanocomposites

Abderrahmane Habi,[1,2] Said Djadoun,[1] Yves Grohens[3]

[1]*Laboratoire de matériaux polymères, Faculté de chimie, Université des sciences et de la technologie Houari Boumediene, BP 32, El Alia, Algiers 16111, Algeria*
[2]*Laboratoire de chimie organique industrielle, Faculté des sciences et sciences de l'ingénieur, Université Abderrahmane MIRA, Béjaïa 06000, Algeria*
[3]*Laboratoire Polymères, Propriétés aux Interfaces et Composites, Rue Saint Maudé, LORIENT Cedex BP 92116 - 56321, France*

Received 18 June 2008; accepted 30 March 2009
DOI 10.1002/app.30536
Published online 2 June 2009 in Wiley InterScience (www.interscience.wiley.com).

ABSTRACT: Poly(styrene-*co*-methacrylic acid) containing 29 mol % of methacrylic acid (SMA-29) and poly(isobutyl methacrylate-*co*-4-vinylpyridine) containing 20 mol % of 4-vinylpyridine (IBM4VP-20) were synthesized, characterized, and used to elaborate binary and ternary nanocomposites of different ratios with a 3% by weight hexadecylammonium-modified bentonite from Maghnia (Algeria) by casting method from tetrahydrofuran (THF) solutions. The morphology and the thermal behavior of these binary and ternary elaborated nanocomposites were investigated by X-ray diffraction, scanning electron microscopy, FTIR spectroscopy, differential scanning calorimetry, and thermogravimetry. Polymer nanocomposites and nanoblends of different morphologies were obtained. The effect of the organoclay and its dispersion within the blend matrix on the phase behavior of the miscible SMA29/IBM4VP20 blends is discussed. The obtained results showed that increasing the amount of SMA29 in the IBM4VP20/SMA29 blend leads to near exfoliated nanostructure with significantly improved thermal stability.
 J Appl Polym Sci 114: 322–330, 2009

Key words: poly(styrene-*co*-methacrylic acid); poly-(isobutyl methacrylate-*co*-4-vinylpyridine) x-ray diffraction; thermal degradation; DSC; miscibility; nanocomposite and nanoblends

INTRODUCTION

The interest in polymer-clay nanocomposites has increased significantly over the past two decades. These materials may particularly exhibit improved thermal stability and mechanical properties, reduced flammability, and better barrier properties compared with conventionally filled polymers.[1–3] The effective dispersion of the clay within the polymer matrix is mainly responsible for the improvement of such properties. Depending on the interactions that occurred between the polymer matrix and the nanoparticle, two types of nanocomposites are in general produced, such as intercalated or exfoliated. The exfoliated structure is, in general, more effective in improving the properties of the resulting material.

Blending two polymers may be a relatively cheap and effective way of elaborating materials with improved properties for a specific end use. However, this method is limited in industry because most pairs of polymers are thermodynamically immiscible with each other, generally leading to poor mechanical properties. Tough extensive research has been recently carried out on polymer-clay nanocomposites; only a limited number of articles have reported on ternary nanocomposites of binary blends of polymers or copolymers with clays.[4–8]

Some authors have reported that organically modified clays could play a role as a compatibilizer for immiscible polymer blends.[9–11]

Polystyrene (PS) is one of the quantitatively most important thermoplastics largely used in packaging. As reported in the literature, some of its properties such as oxygen diffusion, flammability, and mechanical properties need to be improved.

The incorporation of 29 mol % of methacrylic acid by random copolymerization within the polystyrene matrix significantly increased its glass transition temperature and somehow delayed its thermal stability.[12]

Poly(isobutyl methacrylate) (PIBMA) is mostly of poly(alkyl methacrylate) of low thermal stability and has a lower glass transition temperature than PS or SMA29. Blending PIBMA with PS or SMA29 did

Correspondence to: S. Djadoun (matpolylab@yahoo.fr).

not, however, improve the thermal stability of the resulting mixture as phase separation occurred.[13]

In a previous study, we have showed that depending on the nature of the solvent used and the density of interacting species, methacrylic acid and 4-vinylpyridine, incorporated within PS and PIBMA matrices respectively, miscible blends or interpolymer complexes SMA/IBM4VP were formed.[12] In addition, it also showed that interpolymer complexes based on poly(styrene-*co*-methacrylic acid) containing 29 mol % of methacrylic acid (SMA29) and poly(isobutyl methacrylate-*co*-4-vinylpyridine) containing 20 mol % of 4-vinylpyridine (IBM4VP20) exhibited better thermal stability as compared with their corresponding blends, mainly due to the presence of stronger specific interactions that occurred between the carboxylic groups of the SMA29 and the 4-vinylpyridine of the IBM4VP20.

Polymer-layered silicate nanocomposites can be synthesized by *in situ* polymerization or polymer intercalation from solution or melt.[14–16]

Previously synthesized and characterized SMA29 and IBM4VP20 were used to elaborate binary and ternary nanocomposites from these copolymers and their blends of different ratios with an hexadecylammonium-modified bentonite from Maghnia (Algeria) by casting method from THF solutions. The present study focuses on the analysis of the morphology and the thermal behavior of these binary and ternary elaborated nanocomposites by X-ray diffraction (XRD), scanning electron microscopy (SEM), differential scanning calorimetry (DSC), and thermogravimetry (TGA).

EXPERIMENTAL

Materials

Poly(styrene-*co*-methacrylic acid) containing 29 mol % of methacrylic acid (SMA29) and poly(isobutyl methacrylate-*co*-4-vinylpyridine) containing 20 mol % of 4-vinylpyridine (IBM4VP20) were prepared by free radical polymerization and characterized in our laboratory as described previously.[12] The intrinsic viscosities of these copolymers determined at 25°C in THF using a Ubbelohde viscometer were 0.79 and 1.20 dL/g for SMA29 and IBM4VP20, respectively.

The chemical composition of pure bentonite (PBT) from Maghnia, kindly supplied by Bentonite Company of Algeria, determined by the central laboratory of the ENOF using X-ray fluorescence is SiO_2 (55–65%) Al_2O_3 (12–18%) Fe_2O_3 (1–3%) Na_2O (1–3%) CaO (1–5%) K_2O (0.76–1.75%) MgO (2–3%). This analysis indicates that this clay is a montmorillonite type.

Preparation of organo-bentonite clay (OBT)

Hexadecylammonium chloride was prepared by mixing appropriate amounts of hexadecylamine with concentrated HCl in 150 mL of distilled water and then added to an already separately dispersed bentonite into the hot clay–water mixture at 80°C and stirred vigorously for 1 h. The mixture was then filtered and washed with water in ethanol (50/50 vol %) until negative chloride test was obtained using $AgNO_3$. The hexadecylammonium-exchanged clay (OBT) was then dried at 75°C for 3 days in a vacuum oven and kept in a dessicator.

Preparation of binary and ternary blend nanocomposites

SMA29/OBT, IBM4VP20/OBT, and IBM4VP20/SMA29/OBT systems were prepared by solution intercalation method using THF as the solvent for these copolymers, their (65/35 and 50/50) blends and the dispersing medium for clay particles. SMA29 and IBM4VP20 copolymers, SMA29/IBM4VP20 blends, and the OBT were separately dissolved in THF to form dilute solutions during 24 h. The OBT/THF solution was then added to the dissolved copolymers and their blends of different compositions. After solvent evaporation, the obtained materials (films) are dried to constant weight in a vacuum oven at 60°C during 5 days to remove any trace of solvent. All these materials were characterized by FTIR, XRD, SEM, DSC, and TGA.

X-ray diffraction

X-ray diffraction patterns of the pure bentonite, OBT, the two copolymers, their virgin polymer blends, and their ternary nanocomposites were obtained from a Philips PW3710 diffractometer in the range of 2θ (1.5-50°). The Monochromatic radiation applied was Cu Kα (1.5406 Å) operating at 35 kV and 25 mA.

SEM

The morphology of the SMA29 and IBM4VP20 copolymers, their (65/35 and 50/50) pristine blend compositions and their IBM4VP20/SMA29/OBT nanocomposites were investigated from fractured surfaces of samples in liquid nitrogen using a JEOL JSM 6460 LV scanning electron microscope.

DSC

The glass transition temperatures (T_g) of the synthesized pure and organo-modified copolymers, their pristine blends and their nanoblends were determined by differential scanning using a Pyris 1 Perkin Elmer DSC under nitrogen at 20 K/min.

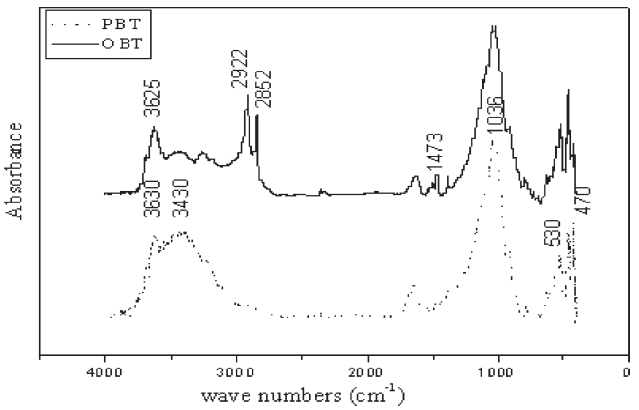

Figure 1 FTIR spectra of PBT and organo-bentonite clay (OBT).

TGA

Thermogravimetric experiments were carried out with a SETARAM TGA 92 thermal analyzer using a scanning rate of 10°C/min under nitrogen from room temperature to 500°C.

FTIR

FTIR spectra of pure and organically modified bentonite specimens prepared by mixing a small amount of clay with spectroscopic KBr and of thin films of pristine blends and of ternary nanocomposites cast from THF solutions onto KBr disks were recorded at 2 cm^{-1} resolution and 60 scans on a BIORAD spectrometer.

RESULTS AND DISCUSSION

We have previously showed that miscible blends and interpolymer complexes were separately obtained when SMA29 and IBM4VP20 are mixed together in THF or butanone, mainly due to the presence of strong specific interactions that occurred between the carboxylic groups of the SMA29 and the 4-vinylpyridine of the IBM4VP20.[12]

We have also studied the phase behavior of the IBM4VP20/SMA29 system in the whole composition range. The T_g-composition variation of this system showed that the most important deviation of T_g of the blend from the weight average occurred in the 40–60% composition range. The complexation yield of this system reached its maximum in butan-2-one around 1 : 1 ratio. Based on these results, this investigation then focuses on these compositions that led to the most improved properties of the virgin blends.

In this study, we have carried out an investigation not only on the effect of modified Maghnia bentonite (OBT), miscibility, morphology, and thermal stability of these blends but also aimed to contribute to the comprehension of the very complex intercalation mechanism of nano blends in solution.

To confirm the modification of the bentonite, we have characterized the pure and modified clays by FTIR and XRD. Figure 1 shows the FTIR spectra of these clays.The new bands observed with the modified bentonite at 2922 cm^{-1}, 2852 cm^{-1}, and 1473 cm^{-1} indicate the intercalation of the salt molecules into the clay structure. The peak at 1036 cm^{-1} characterizes the Si-O groups of the clay. The peak at 3430 cm^{-1} related to water is affected by the organo-modification of the bentonite.

X-ray diffraction

Figure 2 displays the XRD patterns of the PBT and OBT containing 3 wt % of clay. The XRD pattern of the PBT showed a peak at approximately $2\theta = 6.60°$,

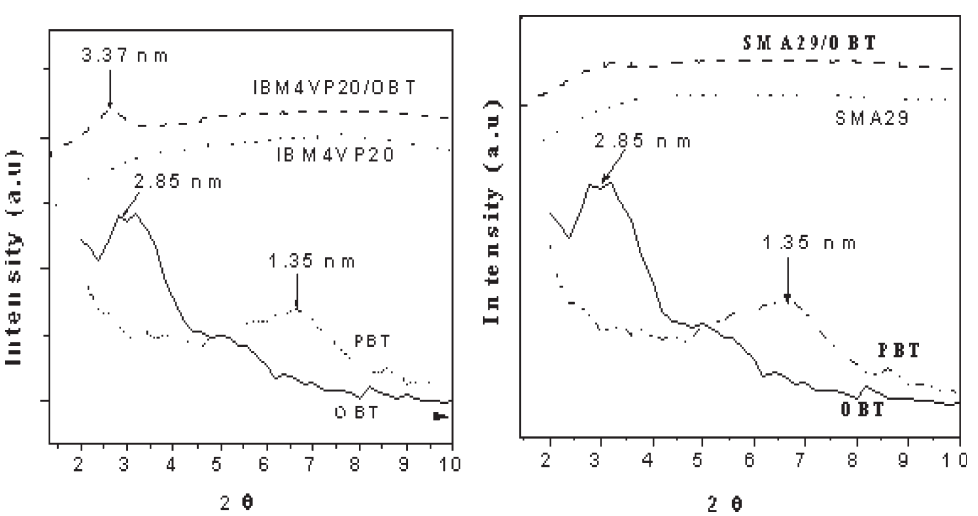

Figure 2 XRD patterns of pure bentonite (PBT), organo-bentonite clay (OBT), (IBM4VP20) (SMA29), (IBM4VP20/OBT), and (SMA29/OBT) containing 3% by wt of OBT.

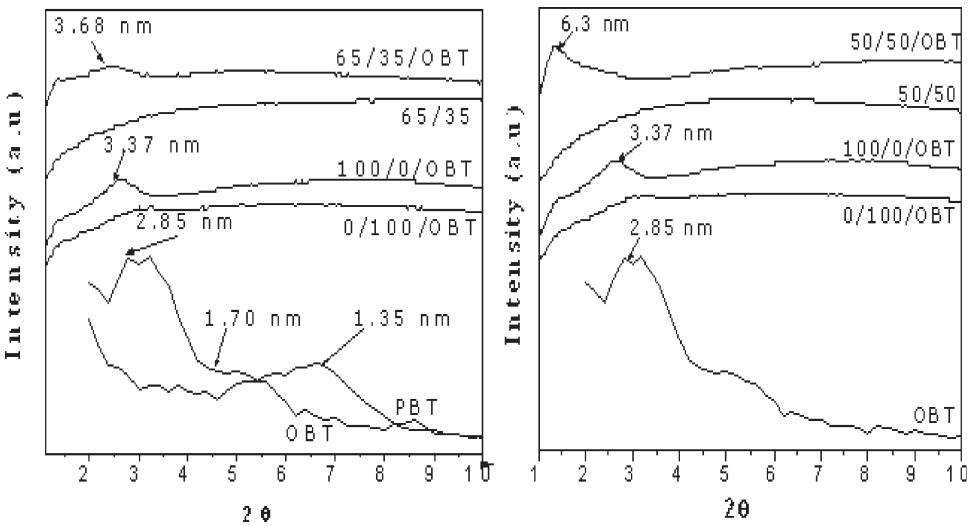

Figure 3 XRD patterns of pure bentonite (PBT), IBM4VP20/SMA29 pristine blends, organo-bentonite clay (OBT), IBM4VP20/OBT (100/0/OBT), SMA29/OBT (0/100/OBT), and IBM4VP20/SMA29/OBT containing 3% by wt of OBT.

which corresponds to a basal spacing of 1.35 nm, whereas a strong peak at $2\theta = 3.10^\circ$ (a basal spacing of 2.85 nm) and a weak peak at $2\theta = 5.20^\circ$ are observed with the OBT. This indicates that the clay layers are widely separated by the hexadecylammonium ions, and that a portion of clay layer was not intercalated.

The degree of interaction of the modified bentonite with each copolymer matrix and selected 35 : 65 and 50 : 50 SMA29/IBM4VP20 blends was first analyzed by X-ray diffraction.

As shown in Figure 2, the presence of OBT in IBM4VP20 appeared as a weak peak at a lower angle ($2\theta = 2.62^\circ$) corresponding to a d-spacing of 3.37 nm, which suggests the formation of an intercalated nanocomposite due to the large d-spacing of the clay that permits the polymer chains to intercalate between the clay layer.

The very weak diffraction peak observed at $2\theta = 3.2^\circ$ for SMA29/OBT may be considered as a formation of a mixed intercalated/exfoliated nanocomposite due to stronger interactions that may occur between the SMA29 chains and the modified clay. These results indicate a better dispersion of the modified bentonite in SMA29 matrix. The weak peak also suggests that some clay layers are not totally intercalated by the polymer chains.

The role of organo-modified bentonite on miscible IBM4VP20/SMA29 blends, as cast from THF is investigated. The choice of this pair of copolymers is based on the results reported earlier that showed that SMA29 chains nearly exfoliate the organo-modified bentonite layers, whereas IBM4VP20 chains intercalate them only.

XRD analyses were carried out for the virgin IBM4VP20/SMA29 blends and their corresponding modified Maghnia bentonite nanocomposites. Figure 3 shows their XRD patterns.

As 35% by weight of SMA29 was added to the IBM4VP20 matrix, the (65/35) IBM4VP20/SMA29/OBT nanocomposite showed a very weak and diffuse peak appearing at a lower angle than that of the IBM4VP20/OBT nanocomposite. This may be attributed to an intercalation of the two polymers of the blends into the clay galleries evidenced by an increase of the d-spacing of the OBT from 2.85 to 3.68 nm.

A near exfoliated structure is, however, observed with increasing the SMA29 composition in the blend as for the 50/50 blend ratio, evidenced from the characteristic peak of the OBT appearing at lower angle corresponding to a d-spacing of 6.30 nm. This shows that the structure of the polymer blend nanocomposite is governed by a contribution from both copolymers of the blend.

SEM

The scanning electron microscopy (SEM) was used as a first step to evaluate the dispersion of the modified bentonite in the IBM4VP20/OBT and SMA29/OBT nanocomposites. Figure 4 shows the micrographs after liquid nitrogen fracture of the copolymers and their corresponding nanocomposites. Significant differences between the SEM images of the virgin copolymers and their corresponding nanocomposites were observed.

Under this magnification, the clay particles can be seen almost evenly dispersed within the IBM4VP20 matrix structure with the presence of small agglomerates (size 0.7 μm). The sizes of these clay particles are in the range of 0.2–0.5 μm.

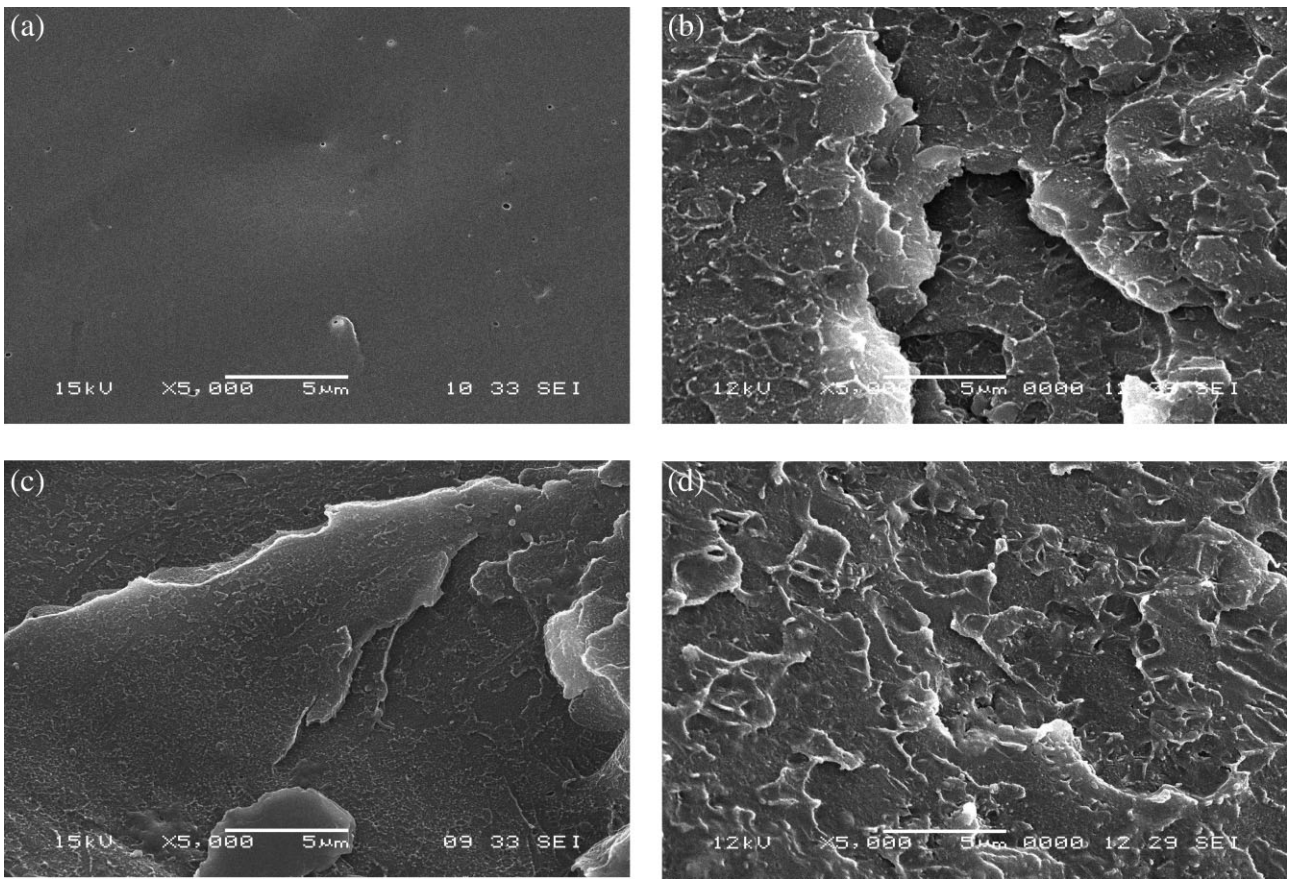

Figure 4 SEM micrographs of (IBM4VP20) (a), (IBM4VP20/OBT) (b), (SMA29) (c), and (SMA29/OBT) (d) containing 3% by wt of OBT.

Better OBT dispersion is observed within SMA29 polymer matrix due to the presence of stronger interactions between the modified bentonite and this copolymer.

Indeed, only a small number of the OBT particles of reduced size (0.1–0.2 μm) homogeneously and finely dispersed in the SMA29 matrix are observed under the same magnification. Due to incomplete intercalation of OBT, some agglomerates of smaller sizes (0.3–0.5 μm) are also observed. These results, in agreement with those obtained by XRD, confirm the formation of "exfoliated-intercalated" SMA29 and intercalated IBM4VP20 nanocomposites.

Complementary morphological informations may be obtained by transmission electron microscopy. Although this technique is used in most cases to characterize the dispersion of the clay in the nanocomposites and nanoblends, it may not be necessary for all systems, and SEM could be sufficient to observe aggregates or clay particles of dimensions as in our systems. Our SEM results revealed significant change in the morphology of the studied blends in the presence of OBT.

This SEM investigation was then extended to ternary nanocomposites, and Figure 5 compares the SEM images of the cryogenically fractured surface of the (65/35) IBM4VP20/SMA29 virgin blend to its hexadecylammonium-modified Maghnia bentonite nanoblend. The homogeneous phase observed with the virgin blend is an evidence of the miscibility of these two copolymers. Under the same magnification, clay particles can be seen almost evenly dispersed within a homogeneous nanoblend matrix structure with the presence of small agglomerates. The average sizes of these clay particles are in the range of 0.2–0.5 μm, smaller than that of the IBM4VP20 nanocomposite.

Such agglomerates are not observed with the (50/50) organically modified nanocomposite. Only small size clay particles homogeneously and finely dispersed in the polymer blend matrix are observed under the same magnification. These results, in agreement with those of the XRD analysis, confirm the miscibility of both blends and nanoblends of different ratios and that the dispersion of OBT within the nanoblend depends on the composition of the blend.

TGA analysis

The thermal stability of the pure copolymers and of their corresponding nanocomposites was examined by thermogravimetry (TGA). Figure 6 shows their TGA and d(TGA) curves measured under nitrogen

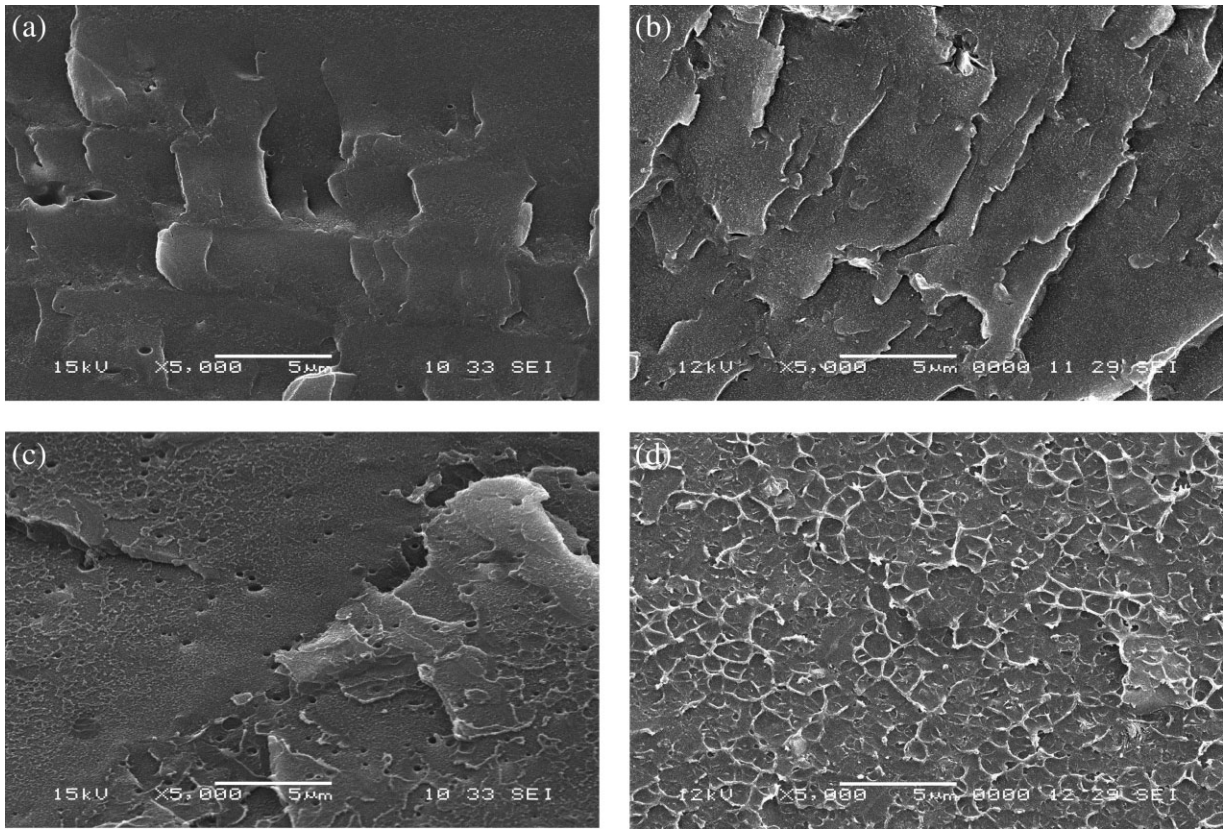

Figure 5 SEM micrographs of IBM4VP20/SMA29 blends (a: 50/50, b: 65/35) and of their corresponding IBM4VP20/SMA29/OBT nanoblends containing 3% by wt of OBT (c, d).

atmosphere, whereas Table I summarizes their thermogravimetric parameters with T_{10} and T_{50} the temperatures at which 10%, 50% degradation occurs, respectively. T_{max} is the temperature at maximum degradation, determined from the corresponding derivative curve.

Both IBM4VP20 and SMA29 copolymers contain hydrophilic moieties and absorb relatively higher amount of water than their corresponding nanocomposites. The release of water is observed in the first step, below the degradation of the salt as evidenced by DTG in the 170–230°C region. Significant thermal

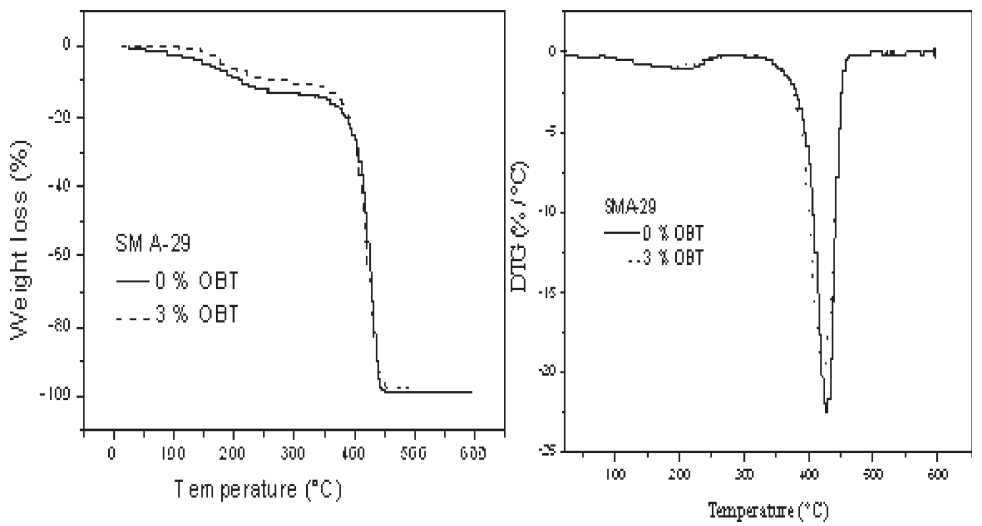

Figure 6 TG and d(TG) curves of SMA29 and SMA29/OBT conducted under nitrogen.

TABLE I
Thermogravimetric Parameters of Copolymers and their Nanocomposites

Materials	T_{10} (°C)	T_{50} (°C)	Td max. (°C)	Char (%)
IBM4VP20	291	354	362	1.8
IBM4VP20/OBT	305	347	348	1.7
SMA29	214	419	415	0.8
SMA29/OBT	296	415	423	2.7

stability improvement is observed with both nanocomposites in this region.

The data given in Table I show that both IBM4VP20/OBT and SMA29/OBT nanocomposites have higher T_{10} than their corresponding pure copolymers. The two nanocomposites, however, displayed different thermal behavior at higher temperatures as shown from their T_{50} and T_{max}.

These nanocomposites displayed lower thermal stability at T_{50} above the degradation temperature of the salt. This lower thermal stability of the nanocomposite may be mainly due to the presence of hexadecylammonium species and other effects as also reported in the literature.

The different degree of dispersion and interactions of OBT with these copolymers affected the overall thermal stability of these latter. The presence of 3% by weight of OBT increased the temperature of degradation of SMA29 as evidenced by a higher char of the nanocomposite while a slightly higher char is observed with the pure IBM4VP20

The improved thermal stability observed with the SMA29/OBT nanocomposite may be attributed to the near exfoliated structure of this nanocomposite and to the barrier effect of the modified bentonite layers that are dispersed in the copolymer matrix.

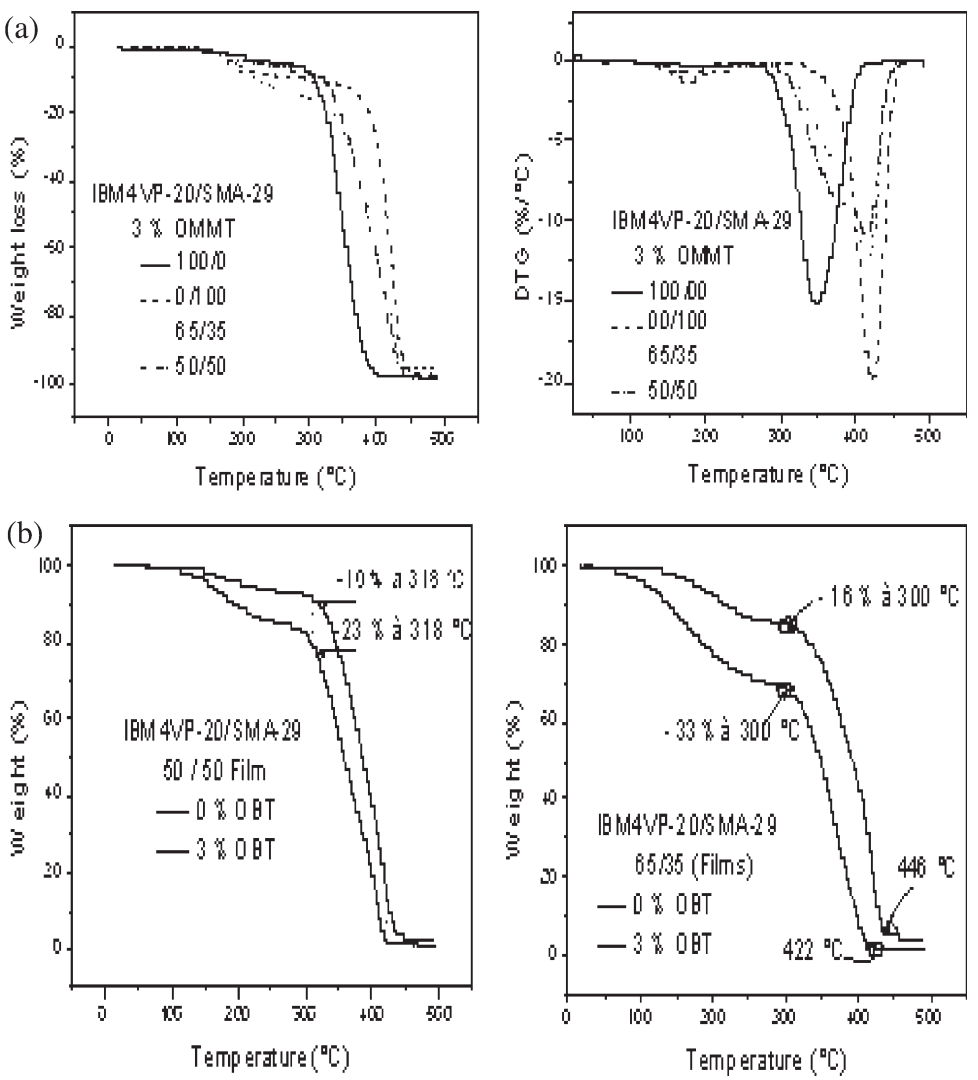

Figure 7 a, TGA and d(TGA) curves of pristine IBM4VP20/SMA29 blends and their corresponding nanoblends containing 3% by wt of OBT, conducted under nitrogen. b, TGA curves of each IBM4VP20/SMA29 blend and its corresponding nanoblend containing 3% by wt of OBT, conducted under nitrogen.

TABLE II
Thermogravimetric Parameters of IBM4VP20/SMA29 Blends and their Corresponding Nanoblends

Materials	T_{10} (°C)	T_{50} (°C)	Td max. (°C)	Char (%)
IBM4VP20/SMA29 (50/50)	194	355	353 et 408	1.05
IBM4VP20/SMA29/OBT (50/50)	318	383	382 et 415	2.80
IBM4VP20/SMA29 (65/35)	141	348	365 et 397	0.80
IBM4VP20/SMA29/OBT (65/35)	218	392	384 et 417	4.10

The incorporation of layered silicates into polymer blends is expected to improve the thermal stability of the resulting ternary nanocomposites.[17–19] Sinha Ray et al.[6] also reported that the thermal stability of the nanoblends is related to the final morphology of the blend.

The thermal stability of the virgin (65/35) and (50/50) IBM4VP20/SMA29 blends and of their OBT/IBM4VP20/SMA29 nanoblends, a property of a high interest, was investigated by TGA under the same conditions than that of their polymer/nanocomposite. Their TGA and d(TGA) curves are shown in Figure 7a, whereas their thermogravimetric parameters are gathered in Table II. The nanoblends showed better thermal stability than the virgin blends. The decomposition temperatures at 10% as well as at 50% weight loss and the temperature at maximum degradation of the nanoblends are higher than that of the virgin blends, as shown in Figure 7b. The amount of char at 500°C also increased slightly.

These results confirm that significant improvements in the temperatures of degradation are observed when 3% by weight of OBT are incorporated within the polymer blend matrices. The intercalated (65/35) IBM4VP20/SMA29/OBT nanoblend showed better thermal stability than both its virgin corresponding blend and the near exfoliated (50/50) nanoblend. This shows that indeed the thermal stability depends on the final morphology as also reported by Sinha et al.[6]

DSC analysis

A DSC analysis was carried out to investigate the effect of OBT on the morphology of the pure copolymers and their blends. We have then determined the glass transition temperature, T_g, of the pure copolymers and of their binary and ternary nanocomposites, as cast from THF. The results displayed in Table III show that the T_g of both polymer nanocomposites increased by 7–8°C compared with their pure copolymers due to attractive interactions that may have occurred between the clay surface and the polymer chains.

We have previously reported[12] that the IBM4VP20/SMA29 blends, as cast from THF were miscible and a single T_g was observed with each blend composition. As shown in Table IV, the single compositionally dependent glass transition temperature observed with these nanoblends is an evidence of their miscibility. The T_g of the nanoblends increased by 7–12°C compared with their corresponding virgin blends due to attractive interactions that may have occurred between the clay surface and the polymer chains.

TABLE III
Glass Transition Temperatures of IBM4VP20, SMA29, and their Corresponding Nanocomposites

Materials	T_g (°C)
IBM4VP20	78
IBM4VP20/OBT	86
SMA29	152
SMA29/OBT	159

FTIR analysis

The OBT is dispersed differently within the individual polymer matrices due to attractive interactions of different strength that occurred between the clay surface and the polymer chains of different nature.

The miscibility of the pristine IBM4VP20/SMA29 blends is mainly due to the presence of sufficient carboxyl-pyridine hydrogen bonding interactions that occurred between the copolymers, as evidenced qualitatively by FTIR spectroscopy from the appearance of a new band at 1607 cm^{-1}, attributed to associated pyridine groups.

The presence of OBT within the blends will affect these latter interactions. Several kinds of interactions of various strengths may occur between the clay and the individual polymer chains or polymer blend.

The FTIR analysis still revealed the presence of hydrogen bonded carboxyl-pyridine interactions occurring between IBM4VP20 and SMA29 within the studied nanoblends as shown in Figure 8. The intensity of the band at 1607 cm^{-1} attributed to associated pyridine groups and characterizing these carboxyl-pyridine interactions decreased as OBT is added to the blend. This indicates that the number of interacting sites between the two copolymers within the nanoblends is less than within the virgin blends. The miscibility of these nanoblends evidenced by the

TABLE IV
Glass Transition Temperatures of Pristine IBM4VP20/SMA29 Blends and their Corresponding Nanocomposites

Materials	T_g (°C)
IBM4VP20/SMA29 (50/50)	110
IBM4VP20/SMA29/OBT (50/50)	122
IBM4VP20/SMA29 (65/35)	99
IBM4VP20/SMA29/OBT (65/35)	110

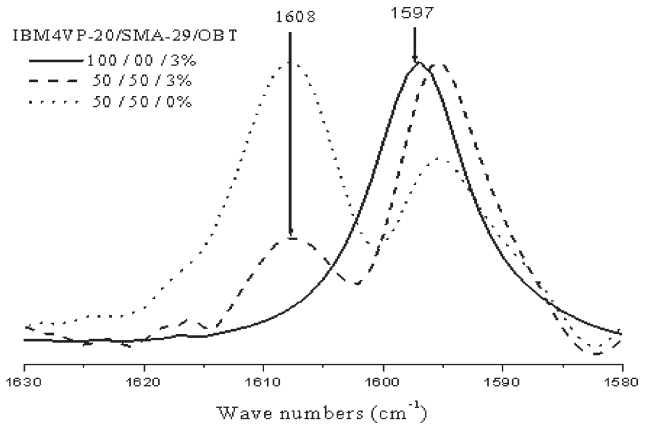

Figure 8 FTIR spectra of IBM4VP20, pristine IBM4VP20/SMA29 (50 : 50) blend, and IBM4VP20/SMA29/OBT (50 : 50) nanoblend containing 3% by wt of OBT in the 1630–1580 cm^{-1} region.

observation of single T_gs higher than the ones of their corresponding virgin blends and the decrease of the density of specific interactions between the two copolymers indicate that stronger interactions may have occurred between the organically modified clay and the polymer blend matrix.

CONCLUSION

Maghnia bentonite (Algeria) was modified with hexadecylammonium chloride and used to prepare IBM4VP20, SMA29 nanocomposites, and IBM4VP20/SMA29 nanoblends by solution intercalation method using THF as the solvent. These nanocomposites were characterized by XRD, SEM, DSC, and TGA.

The intercalation of the two copolymers and of the 65/35 blend into the clay galleries as evidenced by an increase of the d-spacing of the organo-modified bentonite and the near exfoliated structure, confirmed from the quasi absence of the peak characteristic of the clay obtained with increasing the SMA29 composition in the blend as for the 50/50 blend ratio, indicates that the structure of the polymer blend nanocomposite is governed by a contribution from both copolymers of the blend.

The temperatures of degradation and the T_g of the polymer nanocomposites and their nanoblends increased significantly compared with those of pure copolymers and their corresponding blends due to attractive interactions that may have occurred between the clay surface and the polymer chains.

References

1. Sinha. Ray, S.; Okamoto, M. Prog Polym Sci 2003, 28, 1539.
2. Biswas, M.; Sinha Ray, S. Adv in Polym Sci 2001, 155, 167.
3. Ramos Filho, F. G.; Mélo, T. J. A.; Rabello, M. S.; Silva, S. M. L. Polym Degrad stab 2005, 89, 383.
4. Sinha Ray, S.; Bousmina, M.; Maazouz, A. Polym Eng and Sci 2006, 1121.
5. Shah, R. K.; Hunter, D. L.; Paul, D. R. Polymer 2005, 46, 2646.
6. Sinha Ray, S.; Bandyopadhyay, J.; Bousmina, M. Macromol Mater Eng 2007, 292, 729.
7. Li, Y.; Shimizu, H. Macromol Rapid Commun 2005, 26, 710.
8. Li, Y.; Shimizu, H. Eur polym J 2006, 42, 3202.
9. Sinha Ray, S.; Bousmina, M. Macromol Rapid Commun 2005, 26, 450.
10. Yurekli, K.; Karim, A.; Amis, E. J.; Krishnamoorti, R. Macromolecules 2004, 37, 507.
11. Si, M.; Araki, T.; Ade, H.; Kilcoyne, A. L. D.; Fisher, R.; Sokolov, J. C.; Rafailovich, M. H. Macromolecules 2006, 39, 4793.
12. Habi, A.; Djadoun, S. Thermochim Acta 2008, 469, 1.
13. Habi, A.; Djadoun, S. Eur Polym J 1999, 35, 483.
14. Shen, Z.; Simon, G. P.; Cheng, Y. B. Polymer 2002, 43, 4251.
15. Chang, J. H.; Jang, T. G.; Ihn, K. J.; Lee, W. K.; Sur, G. S. J Appl Polym Sci 2003, 90, 3208.
16. Chow, W. S.; Mohd. Ishak, Z. A.; Ishiaku, U. S.; Karger-Kocsis, J.; Apostolov, A. A. J Appl Polym Sci 2004, 91, 175.
17. Wang, Y.; Zhang, Q.; Fu, Q. Macromol Rapid Commun 2003, 4, 231.
18. Xu, Y.; Brittain, W. J.; Varia, R. A.; Price, G. Polymer 2006, 47, 4564.
19. Lee, M. H.; Dan, C. H.; Kim, J. H.; Cha, J.; Kim, S.; Hwang, Y.; Lee, C. H. Polymer 2006, 47, 4359.